JOURNAL OF OPTOELECTRONICS AND ADVANCED MATERIALS Vol 9, No. 9, September 2007, p. 2681 - 2685

Correlation between the electron state density and the electrical resistivity in the nanostructured powder of the Ni-Mo alloy

L. RIBIĆ-ZELENOVIĆ, L. RAFAILOVIĆ, A. MARIČIĆ, M. SPASOJEVIĆ
Joint Laboratory for Advanced Materials of SASA, Section for Amorphous Systems, Technical Faculty Čačak, Svetog Save 65, 32 000 Čačak, Serbia

The nanostructured powders of the $Ni_{95.4}Mo_{4.6}$ and $Ni_{99}Mo_1$ alloys were obtained by the electrochemical deposition from ammonium solutions of nickel and molybdenum salts. The differential scanning calorimetry DSC and measurements of the temperature dependence of the electrical resistivity, magnetic permeability and the thermoelectromotive force were used to examine the structural changes of the powders. The nanocrystalline alloys $Ni_{95.4}Mo_{4.6}$ and $Ni_{99}Mo_1$ were stable up to about 460 K. The thermal stabilization of the alloys take place within the temperature interval of 460 K to 570 K resulting in a decrease in electrical resistivity and increases in magnetic permeability as well as electron state density in the proximity of the Fermi level. The crystallization temperature was dependent upon the current density of powder formation. The nanocrystalline alloy $Ni_{95.4}Mo_{4.6}$ obtained at j = 70 mA.cm^{-2} was crystallized within the temperature interval of 650 K to 840 K, and the $Ni_{99}Mo_1$ alloy was obtained at j = 180 mA cm^{-2} in the 580 K – 950 K interval. The crystallization of the nanocrystalline alloy brought about decreases in the electrical resistivity and magnetic permeability and an increase in the electron state density near the Fermi level. The electrical resistivity decrease recorded during the structural changes is due to an increase in the electron state density in the proximity of the Fermi level as well as to an increase in the mean free path of conduction electrons.

(Received February 26, 2007; revised July 9, 2007; accepted August 24, 2007)

Keywords: Nanostructured alloy, Electron density of states, Electrical properties, Thermal properties, Magnetic measurements

1. Introduction

The development of new technologies and modern scientific and technical progress has been greatly facilitated by an expansion of the development of new materials. In the last few decades, many new materials have been obtained by powder sintering. Nanostructured alloy powders, in particular, due to their specific electrical, magnetic and corrosive properties have been widely applied [1-16]. Powders with specific characteristics can be obtained by electrochemical deposition [8,16-24]. By making an appropriate choice of the composition and temperature of a solution, nature of the cathode, the interelectrode distance, the deposition growth rate, the solution circulation rate and the current density, powders with specific chemical composition can be obtained [8, 16-24]. The deposition current density has a significant effect on the nature of the deposit. At low current densities smooth coatings are formed. Crystal powders develop in the boundary diffusion current range, whereas the nanostructured ones are created at much higher overpotentials [8,16-24]. The nanostructured alloys are in a metastable state, and when heated the process of structural relaxation takes place followed by the process of crystallization, which in turn affects mechanical, electrical, magnetic and other properties of these materials [9, 16]. During the structural relaxation, free volume decreases, on the one hand, causing a decrease in the diffusion mass transfer, and a partial arrangement of the alloy structure takes place, on the other, increasing its readiness to crystallize [6,25,26]. During the crystallization, an arranged structure is formed and significant changes in the physico-chemical properties of the alloy occur. The processes of relaxation and crystallization of the alloy change the electron state density at the Fermi level $N(E_f)$, bringing about changes in the thermoelectromotive force of the thermocouple prepared by the alloy and other metal [27,28].

Nanocrystalline Ni and Mo alloys have been widely applied lately due to good corrosion and heat ressistance and electrochemical activity towards cathodic hydrogen evolution and anodic oxigen evolution [29-33]. Apart from metallurgical way of alloy production, which is very expensive because of high Mo melting temperature, other methods of their obtaining like mechanical alloying, sputtering or electrolytic deposition from water baths seems to be the most convenient method of alloys production.

The aim of this paper was to identify the thermal stability of the electrochemically obtained nanocrystalline $Ni_{95.4}Mo_{4.6}$ and $Ni_{99}Mo_1$ alloys. Investigations were made of the effect of heating on their electrical and magnetic properties and the electron state density at the Fermi level.

2. Experimental

The powder of nickel and molybdenum alloy was electrodeposited on titanium cathode from ammonium solution $NiSO_4 \cdot 7H_2O$ and $(NH_4)_6Mo_7O_{24} \cdot 7H_2O$ [23,24]. The powder was obtained in a 2.0 dm^3 glass electrochemical cell containing a special part with a Lugin capillary and a saturated calomel electrode. The anode

used was a Pt electrode with 10 cm^2 surface area, and the cathode was a titanium plate with a 6.0 cm^2 surface area and thickness of 0.2 cm. The cell was in a thermostat. The working temperature was maintained at 298 ± 1.0 K. The solution was obtained from p.a. chemicals and triple-distilled water. It contained 10.0 g dm^{-3} $NiSO_4 \cdot 7H_2O$, 1.3 gdm^{-3} $(NH_4)_6Mo_7O_{24} \cdot 7H_2O$, 0.43 gdm^{-3} NaCl and 119.6 cm^3 25 % NH_4OH per dm^3. The standard electronic circuitry was used. The nickel and molybdenum alloy powder was deposited galvanostatically at current densities ranging from 50 $mAcm^{-2}$ to 200 $mAcm^{-2}$. Following the electrolysis, the obtained powder was washed several times with distilled water. After being washed with water, in order to prevent oxidation, the powder was washed with 0.1 % benzoic acid solution and dried at 378 K. The chemical composition of the powder was determined by the atomic absorption method.

The crystal structure and grain size of the powders were determined by X-ray diffraction (XRD) analysis. The XRD measurements was performed on a Philips MRD diffractometer using $Cu_{K\alpha}$ radiation.

Crystallization of the powder was investigated by the differential scanning calorimetry (DSC) method. Thermograms were obtained on a Dupont Thermal Analyzer 1090 at a heating rate of 20 K min^{-1} under a flow of pure argon. Investigation of the electrical properties was made using 40 × 1.2 × 0.5 mm samples, obtained by powder pressing under the pressure of 100 MPa. Electrical resistance was measured by the four-point method within the temperature interval of 293 K to 950 K. The measurements were made in an argon atmosphere. Measurements of relative magnetic permeability were performed using a modified Maxwell method, based on the action of an inhomogeneous field on the magnetic sample. The magnetic force measurements were performed with a sensitivity of 10^{-6} N in an argon atmosphere. The pressed powder sample was mechanically coupled to a copper conductor, forming a Cu – Ni_xMo_y thermocouple for measurements of the thermo electromotive force (TEMF). The Cu–Ni_xMo_y couple was placed into a specially designed furnace, while the other end of the sample was submerged into a mixture of water and ice. The thermo electromotive force (TEMF) produced by the thermocouple during the heating process was measured by a voltmeter of 10^{-5} V sensitivity.

3. Results and discussion

The chemical composition, phase structure, the size of crystal grains and the size and shape of powder particles depend on the electrodeposition current density [23, 24]. As shown previously [23, 24], an increase of the deposition current density induced powders with lower Mo content and smaller crystal powder grains. The powder obtained at j = 70 $mAcm^{-2}$ was composed of $Ni_{95.4}Mo_{4.6}$ and crystal grains of about 14 nm on the average, and the powder created at j= 180 $mAcm^{-2}$ was composed of $Ni_{95.4}Mo_{4.6}$ and crystal grains of about 19 nm on the average [23, 24]. The crystal structure is face-centered cubic lattice (FCC) of the molybdenum-nickel solid solution (Fig. 1).

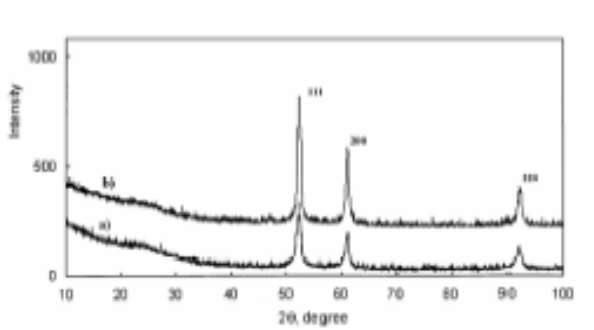

Fig. 1 X ray diffractograms for the a) $Ni_{95.4}Mo_{4.6}$ powder and b) $Ni_{99}Mo_1$.

Apart from the crystal phase, the powder contained an amorphous phase as well. The amorphous phase content increases with an increase of the Mo content [23, 24]. The electrochemically obtained Mo and Ni powders had nanocrystalline structure with many defects. Following the heating of the powders at 750 K and 950 K and cooling down to room temperature, X-ray diffractograms were recorded. The results obtained showed that structural changes occurred during the heating: a) the amorphous phase of the powder transformed into the FCC crystal one; b) the crystal grains of the FCC phase grew to 80.0 nm and c) the number of dislocations and microstrains of the crystal lattice considerably decreased [23, 24].

The structural changes of the electrochemically obtained powders of the Ni and Mo alloys were determined by differential scanning calorimetry (DSC) and by measurements of the temperature dependence of the changes in the electrical resistivity, magnetic permeability and the thermoelectromotive force of the copper/molybdenum-nickel-alloy thermocouple.

Fig. 2 presents the DSC thermogram and temperature dependences of the electrical resistivity and of the relative change of the magnetic permeability of the $Ni_{95.4}Mo_{4.6}$ alloy obtained at j = 70 $mAcm^{-2}$.

The exo-peak occurrence within the temperature interval of 663 K to 873 K in the thermogram presented in Fig. 2 indicated that the powder $Ni_{95.4}Mo_{4.6}$ had nanocrystalline structure.

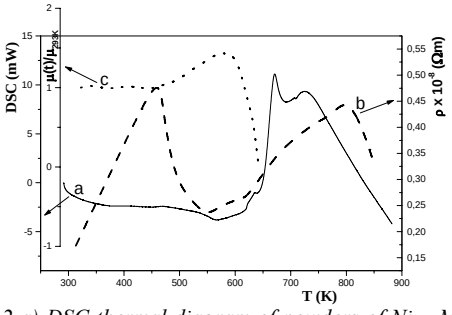

Fig.2 a) DSC thermal diagram of powders of $Ni_{95.4}Mo_{4.6}$ alloy obtained at current density j = 70 $mAcm^{-2}$. Heating rate 20 $Kmin^{-1}$ b) Electrical resistivity as a function of temperature of the pressed powders. Heating rate 30 $Kmin^{-1}$; c) Temperature dependence of relative magnetic permeability of the powders. Heating rate 30 $Kmin^{-1}$.

During heating of the $Ni_{95.4}Mo_{4.6}$ powder in the temperature range from 293 K to 460 K, the magnetic permeability of the alloy did not change and no significant changes were recorded in the thermogram (Fig. 2). This is an indication that in this temperature interval structural changes in the powder did not take place. The linear resistivity increases in the temperature interval concerned (from 293 K to 463 K) confirmed the fact that structural changes did not take place in the alloy. Within the temperature interval of 460 K< T <570 K the resistivity of the $Ni_{95.4}Mo_{4.6}$ alloy decreases and relative magnetic permeability increases. In this temperature interval a weakly pronounced endo-peak was recorded in the thermogram (Fig. 2), indicating that the structural relaxation process take place. The linear resistivity increase in the 620 K to 680 K temperature range indicated that, in this interval, no significant structural change of the powder occurred. The Curie temperature of the powder $Ni_{95.4}Mo_{4.6}$ is 663 K.

The diagrams presented in Fig. 2 shows that the structural change of the $Ni_{95.4}Mo_{4.6}$ powder take place in the 650 K to 840 K temperature interval. In the 690 K to 800 K temperature interval, the increase in electrical resistivity was slowed down with the temperature increase due to partial powder crystallization. In the 800 K to 840 K temperature interval, a sudden decrease in electrical resistivity occurred. In this temperature interval the major part of the alloy crystallized. Following heating of the sample at 840 K, the sample was maintained at this temperature for 30 minutes in order to get the complete crystallization. The sample was then cooled down and its resistivity was measured. The resistivity linearly decreased with the temperature decrease. During further heating of the sample from room temperature to 840 K, the resistivity values obtained were identical to the ones registered during the cooling after the first heating run to 840 K. This is a confirmation that within the temperature interval of 650 K to 840 K, the process of structural change take place and that the $Ni_{95.4}Mo_{4.6}$ powder obtained at j = 70 $mAcm^{-2}$ has nanocrystalline structure.

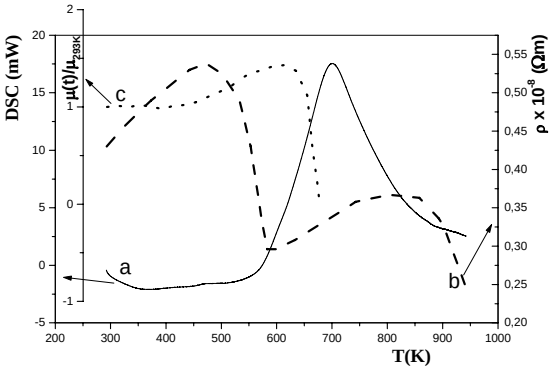

Fig.3 a) DSC thermal diagram of powders of $Ni_{99}Mo_1$ alloy obtained at current density j = 180 $mAcm^{-2}$. Heating rate 20 $Kmin^{-1}$; b) Electrical resistivity as function of temperature of the pressed powders. Heating rate 30 $Kmin^{-1}$. c) Temperature dependence of relative magnetic permeability of the powders. Heating rate 30 $Kmin^{-1}$.

Fig. 3 presents the DSC thermogram and the dependencies of the electrical resistivity and relative change of the magnetic permeability on the temperature of the $Ni_{99}Mo_1$ alloy obtained at j = 180 $mAcm^{-2}$. An analysis of the obtained dependences presented in Fig. 3 indicated that in the 293K <T< 460K temperature interval structural changes in the $Ni_{99}Mo_1$ alloy did not occur. Structural relaxation takes place in the 460 K< T <580 K interval. The $Ni_{99}Mo_1$ powder formed at j = 180 $mAcm^{-2}$ started to crystallize at 580 K, whereas the crystallization of the $Ni_{95.4}Mo_{4.6}$ powder obtained at j = 70 $mAcm^{-2}$ commenced at 650 K. This indicates that the powders evolved at higher current densities were less stable. The crystallization of the $Ni_{99}Mo_1$ nanostructured powder affected its resistivity. In the 690 K< T <790 K temperature interval an increase in electrical resistivity decreased with the temperature increase due to partial crystallization of the alloy. In the 820 K< T < 950 K interval a sudden decline in electrical resistivity occurred. In this temperature interval major part of the alloy crystallized.

Fig. 4 presents the temperature dependence ε (T) of the thermoelectromotive force TEMF of the pressed powder sample of the $Ni_{95.4}Mo_{4.6}$ alloy. The line (—) refers to the temperature dependence of TEMF during the first sample heating to 453 K. After the temperature of 453 K had been reached the sample was maintained at the temperature for 30 minutes and then cooled down to 293 K, following which it was reheated to 453 K. During the latter heating, as in the former one, a completely identical temperature dependence of TEMF was obtained, indicating that in the 293 to 453 K temperature interval structural changes in the alloy did not occur.

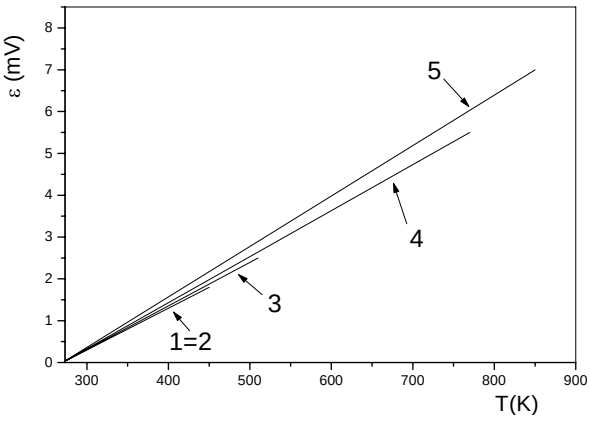

Fig. 4 TEMF temperature dependence of alloy $Ni_{96,4}Mo_{3,6}$ before (1) and after annealing at 453K (2) ; 523K (3); 763K (4); 853K (5). The duration of annealing was 30 min. Heating rate 20 $Kmin^{-1}$. (The powders was obtained at j = 70 $mAcm^{-2}$).

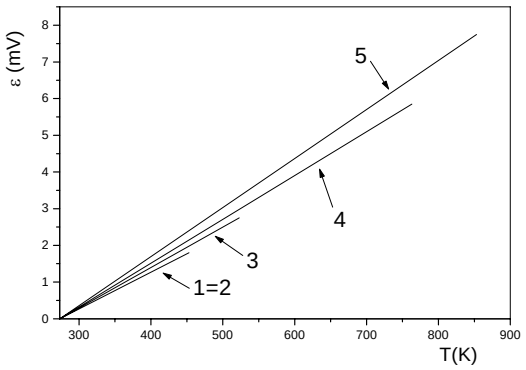

Fig. 5. TEMF temperature dependence of alloy $Ni_{99}Mo_1$ before (1) and after annealing at 453K (2); 523K (3); 763K (4); 853K(5). The duration of annealing was 30 min. Heating rate 20 $Kmin^{-1}$. (The powders was obtained at j = 180 $mAcm^{-2}$).

Following the 30-minute heating of the samples in the temperature range within which structural relaxation take place (523 K) and in the temperature interval where crystallization occurred (763 K and 853 K), the samples were cooled down to 293 K to be subsequently reheated. During the heating linear temperature dependences of TEMF were obtained (Fig. 4). Different coefficients of slopes of these linear dependences indicate structural changes in the samples. The temperature coefficient TEMF is a function of the electron state density at the Fermi level:

$$\alpha = \frac{h^2}{2m_e}\left(\frac{3}{8\pi}\right)^{2/3}\left(N_{1(E_F)}^{2/3} - N_{2(E_F)}^{2/3}\right) \qquad (1)$$

where h is – Planck's constant, m_e – mass of electrons, $N_{1(EF)}$ – electron state density in copper and $N_{2(EF)}$ – electron state density in the $Ni_{95.4}Mo_{4.6}$ alloy. The electron state density in copper remained practically unchanged during heating to 1000 K. The change in the temperature coefficient of TEMF after heating of the sample at specific temperature was caused by the change in the electron state density at the Fermi level in the nanostructured alloy. Based upon the change in the temperature coefficient of the direction, the relative change in the electron state density of the powders caused by the structural relaxation process was determined to be $\frac{\Delta N_{rel}}{N_1}$ =5.0 %. The relative change in the electron state density of the $Ni_{95.4}Mo_{4.6}$ alloy caused by crystallization was $\frac{\Delta N_{cr}}{N_1}$=15.0 %. The overall change in the electron state density caused by structural relaxation and crystallization was $\frac{\Delta N_o}{N_1}$=20.0 %.

Fig. 4 shows the temperature dependence of the TEMF of the pressed powders sample of the $Ni_{99}Mo_1$ alloy. Based upon the obtained experimental dependences presented in Fig. 4, using the changes in the temperature coefficient of the direction, the relative change in the electron state density caused by the structural relaxation process was determined: $\frac{\Delta N_{rel}}{N_1}$ = 4.8 %. The relative change of the electron state density caused by crystallization was $\frac{\Delta N_{cr}}{N_1}$ = 21.9 %. The overall change in the electron state density caused by both structural relaxation and crystallization was $\frac{\Delta N_o}{N_1}$ = 26.7 %.

4. Conclusions

The electrochemically obtained nanostructured alloys $Ni_{95.4}Mo_{4.6}$ and $Ni_{99}Mo_1$ are stable up to 463 K. Thermal stabilization of the alloys takes place in the 463 K to 573 K temperature interval with the decrease in the electrical resistivity and increase in magnetic permeability and electron state density near the Fermi level. The $Ni_{95.4}Mo_{4.6}$ and $Ni_{99}Mo_1$ powders crystallized in the temperature intervals from 663 K to 873 K and from 573 K to 950 K, respectively. The powder crystallization caused a decrease in electrical resistivity and magnetic permeability and an increase in the electron state density in the proximity of the Fermi level. The electrical resistivity decrease during the structural changes is due to an increase in both the electron state density near the Fermi level and the mean free path of conduction electrons.

Acknowledgements

This work was financially supported by the Ministry of Science and Environmental Protection of the Republic of Serbia, project number 142011 G. The authors would like to express their gratitude to academician M. M. Ristic for useful suggestions.

References

[1] T. R. Anantharaman, Trans. Tech., Aedermansorf, Switzerland, 1984.
[2] P. Haasen, R. I. Joffe, Amorphous Metals and Semiconductors, Pergamon, London, 1986.
[3] N. F. Mott, E. A. Davis, Electronic Processes in Non-Crystalline Materials, Clarendon Press, Oxford, 1979.
[4] H. Steeb, H. Warlimont, Rapidly Quenched Metals, Elsevier, Amsterdam, 1985.
[5] Yu. A. Kunitsky, V. I. Lisov, T. L. Tsaregradskaya, O. V. Turkov, Science of Sintering: Current Problems and New Trends, Beograd, 319-328 (2003).
[6] L. A. Jakobson, J. Mc. Kittrik, Rapid Solidification Processing, Elsevier, 1994.
[7] M. V. Susic, J. Mat. Sci. **22**, 3011 (1987).

[8] A. Maricic, M. Spasojevic, L. Rafailovic, V. Milovanovic, L. Ribic-Zelenovic, Material Science Forum **453**, 411 (2004).
[9] M. V. Susic, A. M. Maricic, Mat. Chem. and Physics, **19**, 517 (1998).
[10] M. V. Susic, P. V. Budberg, S. P. Alisova, A. M. Maricic, J. Serb. Chem. Soc. 60 (1995).
[11] A. M. Maricic, M. M. Ristic, Science of Sintering **35**, 31 (2003).
[12] M. V. Susic, D. Minic, A. M. Maricic, B. Jordovic, Science of Sintering **28**, 105 (1996).
[13] M. V. Susic, A. M. Maricic, N. S. Mitrovic, Science of Sintering **28**, 189 (1996).
[14] A. M. Maricic, M. M. Ristic, Science of Sintering **28**, 182 (1996).
[15] A. M. Marici, M. V. Susic, M. M. Ristic, J. Serb. Chem. Soc. **62**(8), 643 (1997).
[16] M. Spasojevic, A. Maricic, L. Rafailovic, Science of Sintering **36**, 105 (2004).
[17] A. R. Despic, K. I. Popov, Modern Aspects of Electrochemistry, Vol. 7 Plenum Press, New York, 1972.
[18] N. Ibl, Helv. Chim. Acta, 37 (1954).
[19] K. I. Popov, M. G. Pavlovic, Electrodeposition of Metal Powders with Controlled Particles Grains Size and Morphology in Modern Aspects of Electrochemistry, B. E. Conway, J. O'M. Bockris, R. E. White, Eds., Vol. 24 Plenum, New York, 1973 pp. 299-391.
[20] M. G. Pavlovic, Lj. J. Pavlovic, N. D. Nikolic, K. I. Popov, Materials Science Forum, **352**, 65 (2000).
[21] M. G. Pavlovic, K. I. Popov, E. R. Stojiljkovic, Bulletin of Electrochemistry **14**, 211 (1998).
[22] M. G. Pavlovic, Lj. J. Pavlovic, E. R. Ivanovic, V. Radmilovic, K. I. Popov, J. Serb. Chem. Soc. **66**, 923 (2001).
[23] M. Spasojevic, A. Maricic, L. Ribic-Zelenovic, L. Rafailovic, B. Jordovic, J. Appl. Electrochem. in press.
[24] L. Ribic-Zelenovic, L. Rafailovic, M. Spasojevic, A. Maricic, Science of Sintering (2006) in press.
[25] K. Suzuki, H. Fudzimori, K. Yosamoto, Amorfnye metally, Metallurgiya, Moskva, 1987.
[26] V. E. Egoruskin, N. V. Melnikova, Metalofizika, T. **10**(1), 81 (1988).
[27] A. P. Spak., V. L. Karbovskij, A. N. Jaresko, Metalofizika i noveisie tehnologii, 16. N°3, 32 (1994).
[28] A. P. Spak., V. L. Karbovskij, Bliznij poredak i osobennosti elektronnoj strukturi v amorfnih metalliceskih splavah na osnove 3d metallov. KNMF, (1994) 44.
[29] J. Niedbala, Acta Metallurgica Slovaca **11**, 166 (2005).
[30] J. Niedbala, K. Wykpis, A. Budnick, E. Lagiewka: Archives of Material Science **23**(2), 123 (2002).
[31] Lagiewka E., Budnick A., Niedbala J.: Archives of Material Science **23**(2), 137 (2002).
[32] E. Beltowska-Lehman, Chassaing E.: J. Appl. Electrochem. **27**, 568 (1977).
[33] Y. Zeng, S. W. Yao, X. Q. Cao, H. X. Juany, Z. Y. Zhoni, H. T. Guo Chin. Chem.**15**, 193 (1997).
[34] J. Y. Huot: J. Electrochem. Soc. **136**, 32 (1989).
[35] L. Arul Ray, V. K. Venkatesan: Ins. J. Hydrogen Energy **13**, 215 (1982).
[36] D. Olszak, V. K. Portnoy, H. Matyja: Nanostructure Materials **12**, 621 (1999).
[37] W. Z. Q. Hue: Zhang Xashou, Surface and Coatings Technology **1-2**, 50 (1997).
[38] S. W. Yao, Y. Zeng, H. T. Guo, Surf. Fin. (Chinese) **16**, 9 (1994).
[39] Y. Zeng, S. W. Yao, H. T. Guo, Platinum Surf. Fin. (Chinese) **16**, 9 (1994).
[40] Y. Zeng, S. W. Yao, H. T. Guo, Platinum Surf. Fin. **82**, 64 (1995).
[41] H.Fukusima, T. Akyama, S. Akagi, Trans. Jpn. Ins. Met. 20 (1979) 358.
[42] E. Chassaing, K. V. Quang, R. Wiart, J. Appl. Electrochem. **19**, 839 (1989).
[43] Y. Zeng, S. W. Yao, H. T. Guo, Chin. J. Chem. **15**, 193 (1997).
[44] E. J. Podlaha, D. Landolt, J. Electrochem. Soc. **143**, 855 (1996).
[45] E. J. Podlaha, D. Landolt, J. Electrochem. Soc. **143**, 893 (1996).
[46] E. J. Podlaha, D. Landolt, J. Electrochem. Soc. **144**, 1672 (1997).
[47] Elisa Navarro-Flores, Zhiwen Chong, Sasha Omanovic, Journal of Molecular Catalysis: Chemical **226**, 179 (2005).
[48] Luciana S.Sanches, Sergio H. Dominigues, Claudia E. B. Marino, Lucia H. Mascaro, Electrochemistry Communications **6**, 543 (2004).

*Corresponding author: lenka@tfc.kg.yu